



# Development of Fuses for Protection of Geiger-Mode Avalanche Photodiode Arrays

MICHAEL GRZESIK,<sup>1,2</sup> ROBERT BAILEY,<sup>1</sup> JOE MAHAN,<sup>1</sup> and JIM AMPE<sup>1</sup>

1.—MIT Lincoln Laboratory, Lexington, MA, USA. 2.—e-mail: michael.j.grzesik@gmail.com

Current-limiting fuses composed of Ti/Al/Ni were developed for use in Geiger-mode avalanche photodiode arrays for each individual pixel in the array. The fuses were designed to burn out at  $\sim 4.5 \times 10^{-3}$  A and maintain post-burnout leakage currents less than  $10^{-7}$  A at 70 V sustained for several minutes. Experimental fuse data are presented and successful incorporation of the fuses into a  $256 \times 64$  pixel InP-based Geiger-mode avalanche photodiode array is reported.

**Key words:** Fuse, avalanche photodiode, Geiger-mode, fabrication, photodiode

## INTRODUCTION

Geiger-mode avalanche photodiode (APD) arrays have found use in a variety of photon-counting imaging<sup>1–5</sup> and communications applications.<sup>6,7</sup> When operating in Geiger-mode, APDs are biased above the diode breakdown voltage. Generation of an electron–hole pair, either through absorption of light or through thermal generation can cause the diode to break down, resulting in a rapid rise in current. This signal swing is large enough to directly drive complementary metal–oxide–semiconductor (CMOS) digital logic without the need for external amplifiers.

An issue encountered when hybridizing Geiger-mode APD arrays and readout integrated circuits (ROIC) is the presence of leaky or shorted diodes. If a leaky or shorted diode is electrically connected to a ROIC, when the APD bias voltage is turned on, this high voltage is essentially seen by the ROIC and can either destroy the APD-ROIC assembly or reduce its performance. For arrays with a small number of pixels, occasional leaky or shorted diodes result in a slightly lower yield from fabricated functional array assemblies. For larger arrays with more pixels, the

likelihood of a faulty diode on the array is high. To minimize the likelihood of a shorted or degraded diode being bonded to a ROIC, each diode on the array can be both visually and electrically prescreened, before packaging, to check for defects. After this prescreening, the defective diodes can be spot knocked so they do not make electrical contact with the ROIC. Although fairly effective at mitigating the effects of shorted diodes in APD-ROIC assemblies, this device prescreening and spot knocking process has three primary disadvantages.

- 1 Visually and electrically inspecting each diode is time-consuming and limits array fabrication throughput.
- 2 Electrical probing of the devices may, itself, damage the APD arrays, which then goes undetected.
- 3 Prescreening does not protect against leakage or shorts that may occur after array hybridization, for example those that may be caused by radiation or material fatigue.

To address these issues, a multilayer per-pixel fuse structure was developed.

## EXPERIMENTAL DEVICE FABRICATION AND CHARACTERIZATION

Several sets of experiments were performed to develop fuses with three characteristics:

(Received April 7, 2015; accepted August 7, 2015; published online September 11, 2015)

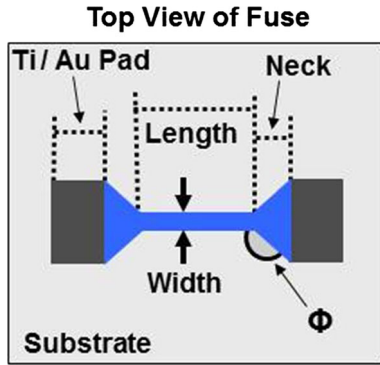


Fig. 1. Schematic diagram of the top view of a fuse structure (not to scale) showing relevant characteristics.

- burnout currents of  $\sim 4.5 \times 10^{-3}$  A;
- leakage currents less than  $10^{-7}$  A at 70 V after the fuse opens; and
- size compatible with array pixel pitches as small as  $20 \mu\text{m}$ .

The purpose of these experiments was, first, to identify an appropriate fuse material, after which the appropriate fuse dimensions (length, width, and neck angle shown in Fig. 1) and metal thicknesses could be determined.

The purpose of the first set of experiments was to identify an appropriate fuse material and the approximate fuse dimensions which would enable the fuses to meet the criteria given above. Initial test fuses were made with a wide range of dimensions. The fuse test structures were fabricated by first spin coating InP substrates with  $\sim 2 \mu\text{m}$  polyimide which was then cured at  $220^\circ\text{C}$  for 1 h in a nitrogen environment. The polyimide layer was then coated with  $2000 \text{ \AA}$   $\text{SiN}_x$  deposited at  $300^\circ\text{C}$  by use of a plasma-enhanced chemical vapor deposition system. Single-layer test fuse structures of different dimensions were then prepared by use of conventional photolithography and electron-beam deposition. Ti, Au, Pt, Al, Si, Ni, and Ge were all examined as potential fuse materials. The final fabrication step was a second photolithography process then electron beam deposition of  $100 \mu\text{m} \times 100 \mu\text{m}$  Ti/Au ( $200 \text{ \AA}/2000 \text{ \AA}$ ) square pads on both ends of the fuse, to be used for electrical probing. The lengths of the first fuses to be tested were from 2 to  $20 \mu\text{m}$  in  $2\text{-}\mu\text{m}$  increments. For each fuse length, fuses were fabricated with widths varying from 2 to  $20 \mu\text{m}$  in  $2\text{-}\mu\text{m}$  increments. For each fuse length–width combination, fuse neck angles of  $90^\circ$ ,  $110^\circ$ ,  $135^\circ$ , and  $160^\circ$  were examined. Test fuses in the first series of experiments consisted of fuses with thicknesses ranging from  $10 \text{ \AA}$  to  $250 \text{ \AA}$  for the different fuse materials.

The burnout currents of the test fuses were determined by performing voltage sweeps in 0.1 V, 200 ms steps while measuring the current. The fuses were measured in series with a  $2 \text{ k}\Omega$  resistor. The burnout current was defined as the highest

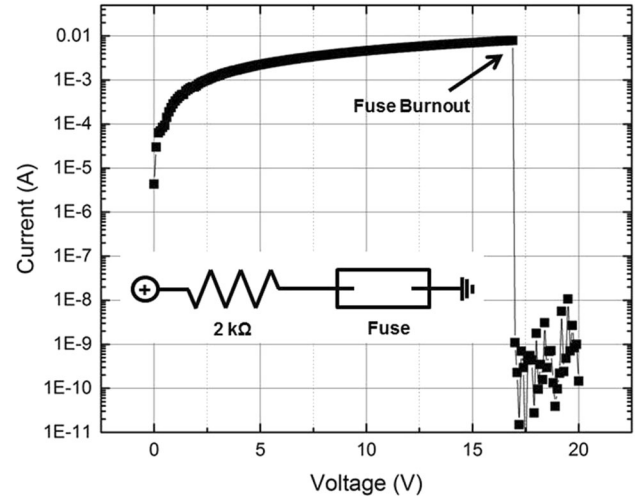


Fig. 2.  $I$ - $V$  measurement for a  $100 \text{ \AA}$  thick Al fuse of length  $2 \mu\text{m}$  and width  $2 \mu\text{m}$ . The inset shows a circuit diagram for the measurement.

current reached before an order of magnitude drop in current (Fig. 2). When studying the different materials as possible fuse materials, it was found that  $\sim 100 \text{ \AA}$  of Al yielded fuses with the appropriate burnout currents, of the order of 5–10 mA, and leakage currents less than  $10^{-7}$  after burnout. It was also observed that test fuses with  $135^\circ$  neck angles and lengths longer than  $4 \mu\text{m}$  were the least likely to burn out away from the center of the fuse, i.e. near the bond pads.

On the basis of the results of the first experiments, a second set of experiments was performed to refine the performance of Al-based fuses. The purpose of these experiments was to enable better understanding of the burnout current of the fuses as a function of length and width, and to make fabrication more compatible with typical APD array fabrication. Reliability issues were also considered. The second set of test fuses was fabricated in the same manner as the first. However, for the test fuses to be more compatible with APD array fabrication, additional metal layers were added to the fuse test structures. In subsequent fuse experiments, a three layer fuse stack was used. The first layer was a  $20\text{-}\text{Å}$  Ti layer deposited to provide adhesion. The second layer, which can be regarded the active fuse material, was an Al layer. The thickness of this layer was varied to adjust the burnout current. The final layer was an Ni cap used to prevent oxidation of the Al layer beneath it.  $20\text{-}\text{Å}$  and  $50\text{-}\text{Å}$  Ni caps were investigated. In addition,  $135^\circ$  and  $142^\circ$  neck angles were studied in the second set of experiments. The measurements for the second set of fuses, again in series with a  $2 \text{ k}\Omega$  resistor, were made by use of an automated probing station. Burnout data were more scattered for fuses with  $50\text{-}\text{Å}$  Ni caps than those with  $20\text{-}\text{Å}$  caps. Burnout currents for fuses with  $135^\circ$  neck angles were slightly lower than for those with  $142^\circ$  neck angles (Fig. 3).

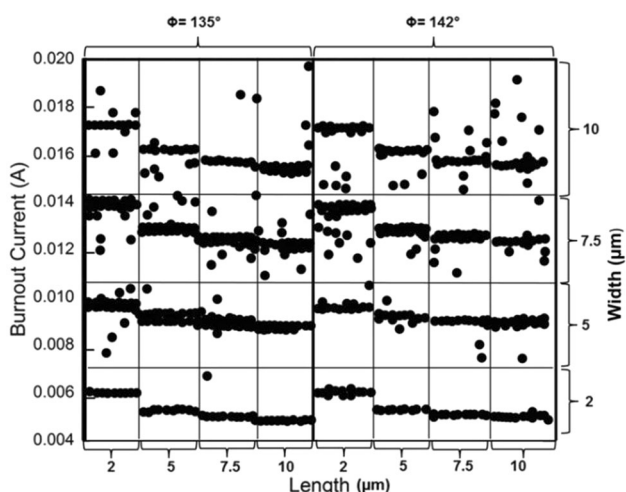


Fig. 3. Burnout current as a function of length, width, and neck angle for Ti/Al/Ni (20/100/50) Å fuses.

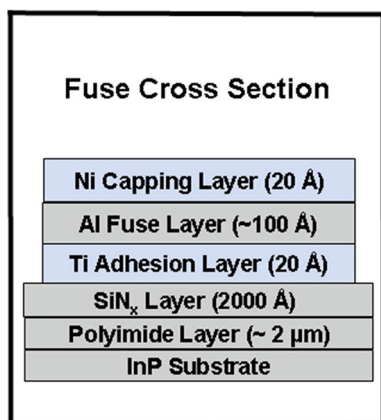


Fig. 4. Schematic diagram of a cross section of the substrate, passivation layer, and Ti/Al/Ni fuse structure used in this work (not to scale).

A third set of experiments was then conducted to refine the fuse burnout current for Ti/Ni/Al fuses. The purpose of these experiments was to enable understanding of burnout current as a function of length, width, and Al thickness. The fuses were fabricated as described for the first two sets of experiments (Fig. 4). In a manner similar to that in the first set of experiments, burnout currents of the fuses in the third set of experiments were measured by voltage sweeping from 0 to 70 V in 0.1 V, 500 ms steps while measuring the current. The fuses were, again, measured in series with a 2 kΩ resistor. The fuses all had 20-Å Ti adhesion layers and 20-Å thick cap layers and 135° neck angles with Al thicknesses of 50, 75, or 100 Å. Fuses from 2 to 8 μm long were measured for 2 and 4-μm widths. The length and widths were measured by use of a microscope with a measurement reticle. Burnout current data from

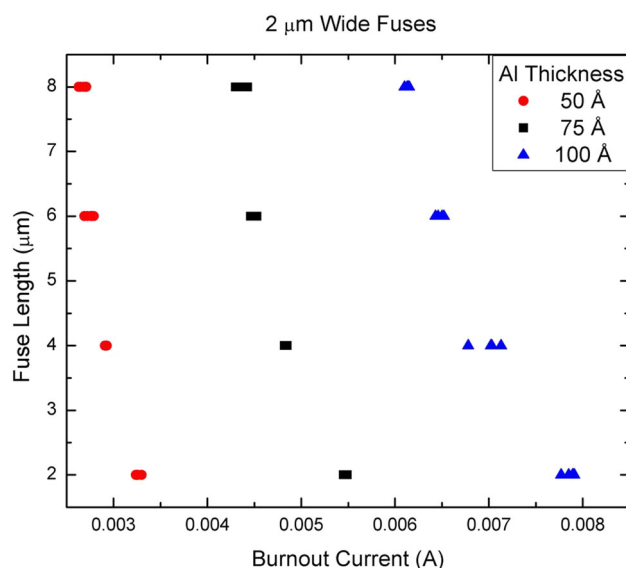


Fig. 5. Fuse burnout current as a function of length and Al thickness for 2-μm wide fuses. For each length–thickness combination, five data points were taken.

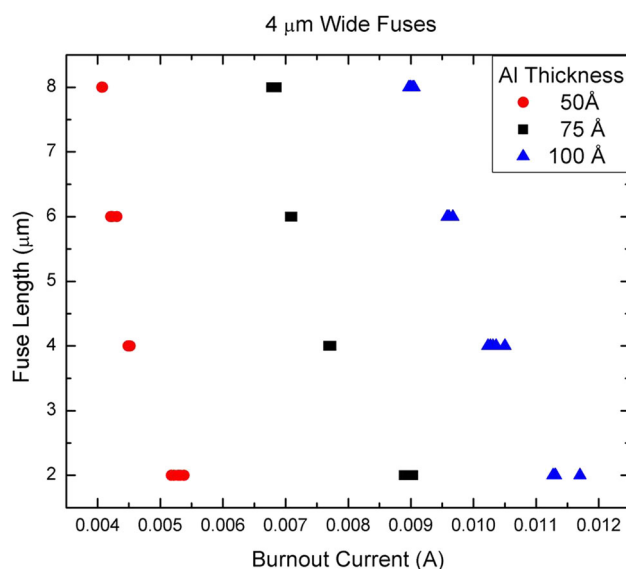


Fig. 6. Fuse burnout current as a function of length and Al thickness for 4-μm wide fuses. For each length–thickness combination, five data points were taken.

the second set of experiments are shown in Figs. 5 and 6.

On the basis of the previous set of experiments, fuses 8 μm long and 2 μm wide (Al thickness 75 Å) with the desired burnout current of  $4.5 \times 10^{-3}$  A were incorporated into a 256 × 64 pixel InP-based Geiger-mode APD array. Without being pre-screened, the fuse-enabled APD array was bump bonded to a ROIC. The array was slowly biased up and brought to an operating voltage of ~68 V. At ~220 s while being biased up, a drop in current was observed indicating a fuse burnout (Fig. 7). The

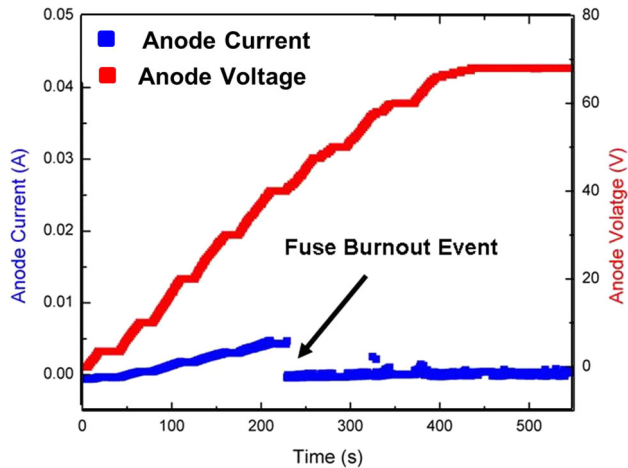


Fig. 7. Anode current and voltage as a function of time while a hybridized  $256 \times 64$  array is being biased up for the first time. At  $\sim 220$  s, a fuse burnout occurs. The array was subsequently brought to standard operating voltage with no deleterious effects from the fuse burnout.

array was successfully biased to  $\sim 68$  V and operated for several hundred seconds with a 4-V over-bias and  $4\text{-}\mu\text{s}$  gate at 20 kHz. Multiple arrays were tested in this manner with some array-ROIC assemblies being separated after operation to verify fuse burnout.

## CONCLUSION

Experiments were performed to develop Al-based fuses with a burnout current of  $\sim 2\text{--}10$  mA. Fuses composed of Ti/Al/Ni ( $20 \text{ \AA}/75 \text{ \AA}/20 \text{ \AA}$ ) were successfully developed and incorporated into a

$256 \times 64$  pixel Geiger-mode APD array. Fuse-enabled APDs are expected to be useful for any type of focal plane array (FPA), particularly linear-mode and Geiger-mode APD arrays, for which a shorted diode can lead to greatly reduced FPA performance. Incorporation of fuses enables increased fabrication throughput and more reliable devices.

## REFERENCES

1. B.F. Aull, A.H. Loomis, D.J. Young, R.M. Heinrichs, B.J. Felton, P.J. Daniels, and D.J. Landers, *Linc. Lab. J.* 13, 335–350 (2002).
2. M.A. Albota, B.A. Aull, D.G. Fouche, R.M. Heinrichs, D.G. Kocher, R.M. Marino, J.G. Mooney, N.R. Newbury, M.E. O'Brien, B.E. Player, B.C. Willard, and J.J. Zayhowski, *Linc. Lab. J.* 13, 351–367 (2002).
3. K.A. McIntosh, J.P. Donnelly, D.C. Oakley, A. Napoleone, S.D. Calawa, L.J. Mahoney, K.M. Molvar, J. Mahan, R.J. Molnar, E.K. Duerr, G.W. Turner, M.J. Manfra, and B.F. Aull, *Proceedings of the 16th Annual Meeting of the IEEE Lasers and Electro-Optics Society*, vol. 2, p. 686 (2003).
4. J.P. Donnelly, E.K. Duerr, K.A. McIntosh, E.A. Dauler, D.C. Oakley, S.H. Groves, C.J. Vineis, J. Mahoney Leonard, K.M. Molvar, P.I. Hopman, K.E. Jensen, G.M. Smith, S. Verghese, and D.C. Shaver, *Proceedings of the 16th Annual Meeting of the IEEE Lasers and Electro-Optics Society*, vol. 42, p. 797 (2006).
5. J.P. Donnelly, K.A. McIntosh, D.C. Oakley, A. Napoleone, S.H. Groves, S. Vernon, L.J. Mahoney, K. Molvar, J. Mahan, J.C. Aversa, E.K. Duerr, Z.L. Liao, B.F. Aull, and D.C. Shaver, *Proc. SPIE* 5791, 281 (2005).
6. D.M. Boroson, R.S. Bondurant, D.V. Murphy, G.S. Mecherle, C.Y. Young, and J. S. Stryjewski, *Proceedings of SPIE Free-Space Laser Communication Technologies XVI*, vol. 5338, p. 16 (2004).
7. S. Verghese, D.M. Cohen, E.A. Dauler, J.P. Donnelly, E.K. Duerr, S.H. Groves, P.I. Hopman, K.E. Jensen, Z.-L. Liao, L.J. Mahoney, K.A. McIntosh, D.C. Oakley, and G.M. Smith, *Proceedings of IEEE Lasers and Electro-Optics Society Summer Topical Meetings*, paper MA2.2, p. 11 (2005).